Definizione stile: BA_Title

Influence of divalent cations in the protein crystallization process assisted by Lanthanide-based additives.

Amandine Roux,[†,‡] Romain Talon,[†] Zaynab Alsalman,[†] Sylvain Engilberge,[†] Anthony D'Aléo,[†] Sebastiano Di Pietro,[†] Adeline Robin,[†] Alessio Bartocci,[†] Guillaume Pilet,[≠] Elise Dumont,[†,⸸] Tristan Wagner, [ς], [ς,¥] Seigo Shima,[ς] François Riobé,[†]* Eric Girard,[†]* Olivier Maury[†]*

† Univ Lyon, ENS de Lyon, CNRS UMR 5182, Laboratoire de Chimie, F-69342 Lyon, France. E-mail: olivier.maury@ens-lyon.fr, francois.riobe@ens-lyon.fr,

‡ Polyvalan Company, F-69342 Lyon, France.

† Univ Grenoble Alpes, CEA, CNRS, IBS, F-38000 Grenoble, France. E-mail: eric.girard@ibs.fr.

≠ Univ de Lyon, CNRS UMR 5615, Université Claude Bernard Lyon 1, 43 boulevard du 11 novembre 1918, F-69622 Villeurbanne cedex.

⸸ Institut Universitaire de France, 1 rue Descartes, 75005 Paris

ς Microbial Protein Structure Group, Max Planck Institute for Terrestrial Microbiology, Karl-von-Frisch-Str. 10, D-35043 Marburg, Germany

¥ Microbial Metabolism Group, Max Planck Institute for Marine Microbiology, 1-Celsiusstrasse, 35043 Bremen, Germany

Supporting Information Placeholder

ABSTRACT The use of lanthanide complexes as powerful auxiliaries for protein crystallization to improve the crucial nucleation and phasing steps, prompted us to systematically analyse the influence of the commercial crystallization kit composition on the efficiency of two lanthanide additives: $[Na]_3[Eu(DPA)_3]$ and Tb-Xo4. This study revealed that the tris-dipicolinate complex presents a lower chemical stability and a strong tendency to self-crystallization detrimental for its use in high-throughput robotized crystallization platform. In particular, crystal structures of $(Mg(H_2O)_6)_3[Eu(DPA)_3]_2{\cdot}7H_2O$ (**1**), $\{(Ca(H_2O)_4)_3[Eu(DPA)_3]_2\}_n{\cdot}11nH_2O$ (**2**) and $\{Cu(DPA)(H_2O)_2\}_n$ (**3**) resulting from spontaneous crystallization in the presence of divalent alkaline-earth cation and transmetallation are reported. On the other hand, the Tb-Xo4 is perfectly soluble in the crystallization media, stable in the presence of alkaline-earth dications and slowly decomposed (within days) by trans-metalation with transition metals. The original structure of $[Tb_4L_4(H_2O)_4]Cl_4{\bullet}15H_2O$ (**4**) is also described. This article also revealed the potential positive of interactions between the crystallization mixture component and Tb-Xo4 leading to the formation of more complex adducts like $\{AdkA/Tb\text{-}Xo4/Mg^{2+}/GOL\}$ in the protein binding sites. The observation of such multi-components adducts illustrated the complexity and versatility of the supramolecular chemistry occurring at the surface of proteins.

Commentato [SDP1]: Positive potential ?

Introduction

During this last decade, the number of protein structures deposited in the Protein Data Bank (PDB https://www.rcsb.org/) has increased steadily despite the emergence of alternative techniques, like NMR or cryoEM and almost 90% of new deposited structures are elucidated using X-ray crystallography. However, this last method still suffers two major chokepoints that severely reduced the efficiency of its implementation: i) the production of high-quality single crystals and ii) the phase determination mandatory for electron density map calculation.[1-2] Actually, the structural genomics statistics estimated that only 10% of the purified proteins will see their structure solved, and consequently a considerable scope for improvement.[3] To tackle these drawbacks, the main stream developments are concentrated in the field of technology with the advancement of structure determination pipelines, more intense radiation sources or the use of XFEL source to address even smaller crystals, and the routine use of high-throughput crystallization platforms to screen an even larger number of conditions with a reduced amount of sample.[4-5] Unfortunately, the certain success of these developments led, in comparison, to neglect the traditional methodological approaches. In particular, the research for new additives that can solved either the crystallization or the phase determination problems or better both simultaneously is a real promising way for improvement in the field for a negligible cost.

Indeed, it is well known that incorporation in a protein crystal of well-ordered heavy atoms enable to solve the phase problem using anomalous-based methods – Single-wavelength Anomalous Dispersion (SAD) and Multi-wavelengths Anomalous Dispersion (MAD).[6] These heavy atoms can be implemented in a covalent way, aspioneered by the Doublié's S-to-Se replacement using selenomethionine, or in a non-covalent one using transition metal salts (Hg, Pt…) or

lanthanide complexes.[7] On the other hand, the development of additives to facilitate the nucleation process was initially focused on heterogeneous compounds like minerals, natural materials such as horse and human hair, nano-porous materials[8-9] and more recently molecular imprinted polymers.[10-11] However, these solid additives are hardly compatible with the generalized homogeneous high-throughput crystallization methods used nowadays.

Figure 1. Selected examples of the three families of soluble

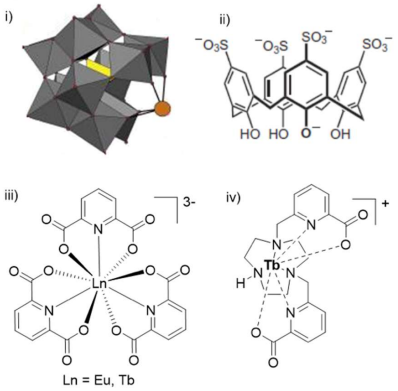

additives used in protein crystallography. (i) Keggin polyoxometalate structure of $[Ce(\alpha\text{-}PW_{11}O_{39})_2]^{10-}$, (ii) p-sulfonatocalix[4]arene (slx4) and lanthanide derivatives studied in this work (iii) tris-dipicolinate $[Na]_3[Ln(DPA)_3]$ and (iv) crystallophore (Tb-Xo4).

Recently, new soluble additives were developed that are fully compatible with the above-mentioned robotized crystallization screening systems (Figure 1): i) the polyoxo-metalates developed by Rompel and co-workers,[12-15] ii) the anionic macrocycles proposed by the team of Crowley (phosphonated or sulfonato-calix[4,6]arenes, cucurbituryl),[16-19] and the lanthanide complexes (iii) tris-dipicolinate[20-21] and iv) crystallophore (Tb-Xo4),[22] reported by our group. All these species can be considered as "molecular glue" inducing a network of supramolecular interactions with proteins in solution and favoring crystalline contacts in the crystal packing. Among these three families of additives, polyoxometalate and lanthanide complexes contain heavy atoms (tungsten, europium or terbium, respectively) and can therefore solve simultaneously the nucleating and the phase determination issues. In particular, based on our own statistics obtained on twenty proteins, the crystallophore increases the number of crystallization conditions by a factor 3-to-7, gives better quality crystals generally suppressing twinning issue and enables de novo phasing in more than 80% of the cases even in complicated ones where selenation was unsuccessful.[23] Furthermore, Tb-Xo4 was also shown to be compatible with micro-seeding, counter-diffusion crystallization methods and serial crystallography (mesh-and-collect method).[23-24] Both $[Na]_3[Eu(DPA)_3]$ and Tb-Xo4 complexes are now available and frequently exploited by the biocrystallographers community to solve the structure of protein of biological interest either for nucleation and/or for phasing steps.[25-31] As a consequence, they have been involved in crystallization processes according to the state-of-the-art high-throughput protocols using pipetting robots, and conventional commercial kits. During the course of these studies, several unexpected results have been obtained suggesting the interaction of the lanthanide complexes with the crystallization condition mixtures that can lead to false positive crystallization results or apparent cooperative behavior favoring the lanthanide complex/protein interaction.

In this article, we described two representative examples of such unexpected results: a false positive observed during the crystallization of the Acriflavine resistant protein B from *Escherichia coli* in the presence of $[Na]_3[Eu(DPA)_3]$, and an apparent cooperative behavior in the crystal structure of adenylate kinase protein from *Methanothermococcus thermolithotrophicus* in the presence of Tb-Xo4. In order to rationalize these results, we explored the behavior of our Ln-based additives in the conventional crystallization kits with a particular focus on the role of divalent alkaline earth or transition metal dications and evidenced detrimental auto-crystallization processes and trans-metalation reactions.

Results and discussions

The crystallization of Acriflavine resistant protein B *from Escherichia coli* (Ec-AcrB), a homotrimeric membrane protein (341 kDa) whose structure was already described (PDB id code: 2GIF), was performed in the presence and in absence of $[Na]_3[Eu(DPA)_3]$ using the High-throughput Crystallization facility (HTXlab, EMBL-Grenoble) with six commercial crystallization kit (see experimental). The drops were regularly imaged to detect the crystallization events and study the effect of the lanthanide additive. A typical comparison is reported in the Figure 2; the protein alone precipitates as an amorphous slurry whereas in the presence of $[Eu(DPA)_3]^{3-}$ exploitable crystals have been obtained that were strongly luminescent under UV-irradiation (Figure 2). However, after analysis, these crystals did not contain any protein and are simply composed of pure $[Eu(DPA)_3]^{3-}$. Consequently, the self-crystallization of such lanthanide complex in the presence of the protein is a typical example of false positive hampering practical co-crystallization experiments with proteins.

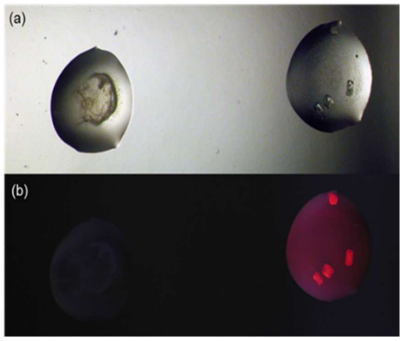

Figure 2. Crystallization drops of Ec-AcrB alone (left) and in the presence of $[Eu(DPA)_3]_3$. (right) in transmission (a) or under 315 nm irradiation (b).

The second unexpected result was obtained during another project where a systematic use of crystallophore on proteins fractions derived from the marine organism *Methanothermococcus thermolithotrophicus* allowed us to solve four unknown protein structures,[23, 30-31] including the adenylate kinase protein (AdkA). The structure of AdkA (PDB id code: 6HF7) was solved at 1.96 Å resolution in a condition containing 50 mM of magnesium ion (see SI for details). The asymmetric unit contains the biological unit consisting in a homo-trimer (Figure 3a) and four bound Tb-Xo4 among which two, with the highest occupancy (0.7) were unambiguously modelled. These latter are located at the same location on two AdkA monomers, and thus involve an identical supramolecular interactions network. The analogous site on third protein monomer is unoccupied. A detailed investigation of the binding pocket reveals the involvement of a hydrated magnesium bridging the crystallophore to the surface protein through aspartate 90 (Figure 3b). The second feature is the presence of a glycerol molecule contained in the protein buffer, completing the coordination sphere of the terbium ion. Starting from this crystal structure, this main binding site was investigated using DFT calculation (see ESI for details). The strongest interaction involves the hydrated magnesium and the aspartate residue (D90) ensuring the binding of the crystallophore to AdkA surface and corresponding to an interaction energy of -25.3 $kcal.mol^{-1}$. This surprising formation of a $\{Tb\text{-}Xo4/Mg^{2+}\}$ adduct in the interaction pocket of AdkA can be compared to the recently reported structure of the protein FprA with the observation of a $\{FprA/Tb\text{-}Xo4/Ca^{2+}\}$ adduct.[32] In both cases, the alkaline-earth cation (Mg^{2+} or Ca^{2+}) was present in the crystallization mixture as well as a glycerol molecule, near Tb-Xo4.

These unexpected and reproducible results prompted us to investigate the behavior of the two complexes $[Na]_3[Eu(DPA)_3]$ and Tb-Xo4 with the different constituents of several commercial crystallization kits routinely used for automated crystallization experiments at the HTXlab (EMBL, Grenoble). These kits encompassed a total of 576 conditions depending on the pH and nature of the buffer (TRIS, MES, HEPES, citric acid, sodium acetate, etc.), the presence of salts at different concentrations (NaCl, $(NH_4)_2SO_3$, $MgCl_2$, $CaCl_2$) or of precipitants (such as polyethyleneglycol, methyl-2,4-pentanediol, isopropanol). In order to evaluate the behavior of our Ln-based additives in such media, the lanthanide complexes were systematically tested alone in the conventional crystallization kits. The experiment was performed by mixing equal volume of the additive solution at the desired concentration (10-100 mM for Tb-Xo4, 25-100 mM for $[Na]_3[Eu(DPA)_3]$) with the crystallization solution to form the sitting drop (Tables S1 and S2). Drops were then evaluated for the presence of potential self-crystallization or precipitate formation by conventional imaging techniques and for the instability of the complexes by the disappearance of the lanthanide emission signal under UV irradiation.

Interestingly, the spontaneous crystallization of $[Na]_3[Eu(DPA)_3]$ was observed in 10% of the conditions at 25 mM and this ratio increased up to 30% at 100 mM. The analysis of these conditions indicated that high concentrations of salt (such as NaCl, $(NH_4)_2SO_3$), typically higher than 0.8 M, the presence of divalent salts (Ca^{2+}, Mg^{2+}) and 2-methyl-2,4-pentanediol or isopropanol favored the self-crystallization of the

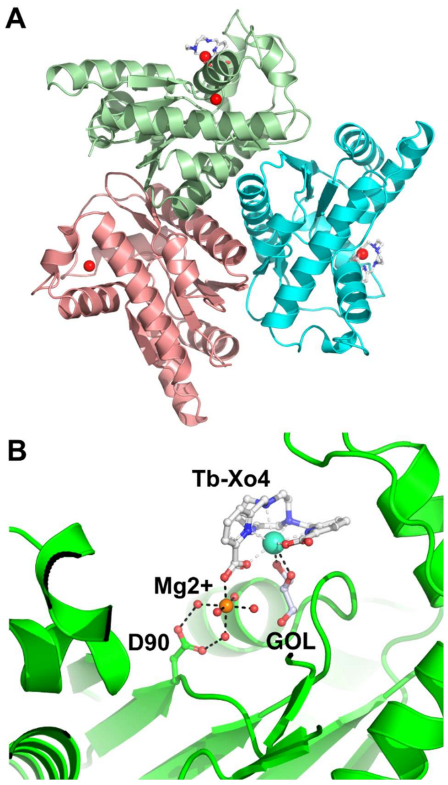

Figure 3. A) Trimer of AdkA co-crystallized with 10 mM Tb-Xo4 (Tb^{3+} in blue) in the presence of $MgCl_2$ (Mg^{2+} in grey); B) Insights into the Tb-Xo4 main binding site.

tris-dipicolinate complex. Even if the increase of the anionic strength or the decrease of the solubility of the complex in the presence of alcohol in the media are classical ways to promote crystallization, the effect of divalent cations was less expected. Therefore, the reactions of $[Na]_3[Eu(DPA)_3]$ with alkaline-earth salts ($CaCl_2$, $MgCl_2$ and $BaCl_2$) were undertaken independently. The slow diffusion of the divalent alkaline earth chloride solutions into an aqueous $[Na]_3[Eu(DPA)_3]$ solution results in

the fast formation of transparent crystals, almost insoluble in water and organic solvent. Diffraction experiments performed on these crystals revealed the formation of structures of respective formula $(Mg(H_2O)_6)_3[Eu(DPA)_3]_2{\cdot}7H_2O$ **1**, $\{(Ca(H_2O)_4)_3[Eu(DPA)_3]_2\}_n{\cdot}11nH_2O$ **2** and of the previously reported $\{[Eu(DPA)_3]_2Ba_3(H_2O)_16]\ 4H_2O\}_\infty$.[33,34-35] Crystal data and refinement parameters are given in Table S3, whereas selected bond lengths are compiled in Tables S4 and S6. In all cases, the Na^+ counter-ion was completely replaced by

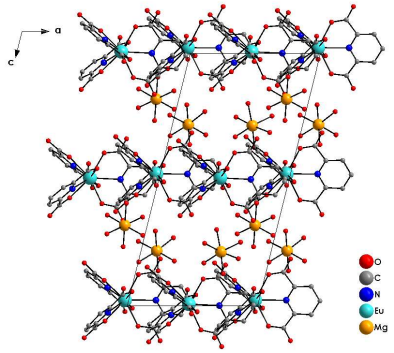

Figure 4. Projection along the b-axis of the unit-cell of the crystal packing of complex **1**, $(Mg(H_2O)_6)_3[Eu(DPA)_3]_2{\cdot}7H_2O$.

$Ca^{2+}/Mg^{2+}/Ba^{2+}$ respectively, which are themselves coordinated by water or by $[Eu(DPA)_3]^{3-}$ carboxylate forming 3-to-2 assemblies with the complex (Figures 4 and 5) and explaining the strong decrease of solubility. While the structure of **1** exhibits isolated $[Eu(DPA)_3]^{3-}$ and $[Mg(H_2O)_6]^{2+}$ units (Figure 4), **2** presents 3D network with $[Eu(DPA)_3]^{3-}$ building blocks connected together through $[Ca(H_2O)_6]^{2+}$ or $[Ca(H_2O)_8]^{2+}$ bridges (Figures 5). In that latter case, an oxygen atom of one (for two ligands) or both (for one ligand) the two DPA carboxy functions complete the Ca^{2+} environment creating links in the three directions between Eu(III) and Ca(II) complexes. The geometric configurations of both complexes were analyzed with the help of SHAPE2.1 program (Tables S5 and S7). The investigation of the precise configurations demonstrated that each Eu^{3+} cations environment within **1** and **2** structures fits well with the nona-coordinate capped square antiprism (CSAPR-9, C_{4v}) and tricapped trigonal prism (TCTPR-9, D_{3h}), respectively. All the Eu-O and Eu-N bond lengths are in good agreement with those observed in the literature.[36-39]

During automated crystallization experiments, we noticed that the characteristic red emission of $[Eu(DPA)_3]^{3-}$ disappeared systematically for all the formulations containing transition metal ions (with M^{2+} = Cd^{2+}, Zn^{2+}, Ni^{2+}, Fe^{2+}, Co^{2+} and mix). Measurements of the $[Na]_3[Eu(DPA)_3]$ emissions were performed in the presence of MCl_2 in diluted water solution ([Ln] = 1 mM, Figure S4). Interestingly, the luminescence of $[Na]_3[Eu(DPA)_3]$ was rapidly quenched after addition of 1 eq. of MCl_2 and about 80% of the emission had disappeared. This competition experiment has also been performed at a concentration closer to the crystallization conditions: slow diffusion of a $CuCl_2$ solution (50 mM) in $[Na]_3[Eu(DPA)_3]$ (50 mM) led to the formation of crystals of $\{Cu(DPA)(H_2O)_2\}_n$ **3** suitable for X-rays diffraction analysis (Figure 6 and Tables S3 and S8). Cu(II) is coordinated to one deprotonated ligand (two oxygen and one nitrogen atoms) and two water molecules. The distorted cation octahedral ML_6 {O5N1} environment is then completed by one oxygen atom (O3) belonging to one neighboring complex unit. This bridge leads to the formation of chains of complexes running along the c-axis of the unit-cell with a $Cu^{2+}{\cdots}Cu^{2+}$ intra-chain distance equals to 3.87 Å. All the Cu-N, Cu-O bond lengths and O-Cu-O, N-Cu-O bond angles are in agreement with those usually listed in the literature for corresponding systems.[40] $\{Cu(DPA)(H_2O)_2\}_n$ chains perfectly stack one above the others in the a-direction of the unit-cell and slightly shifted in the c-direction of the unit-cell. Structural cohesion between chains is assumed by weak interactions (hydrogen bonds and Van der Walls interactions). These results indicated that a trans-metalation reaction occurs very rapidly between $[Eu(DPA)_3]^{3-}$ and transition metal cations leading to the destruction of the lanthanide complex in solution.

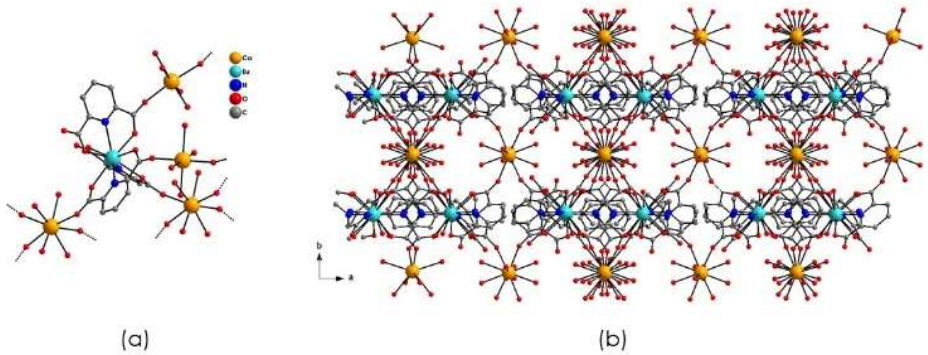

Figure 5. (a) molecular building block of $\{(Ca(H_2O)_4)_3[Eu(DPA)_3]_2\}_n \cdot 11nH_2O$ complex **2**; (b) projection along the c-axis of the unit-cell in order to highlight $[Ca(H_2O)_n]^{2+}$ (in orange) and $[Eu(DPA)_3]^{3-}$ (in blue) planes running perpendicularly to the b-axis of the unit-cell. For clarity, hydrogen atoms and non-coordinated water molecules have been removed.

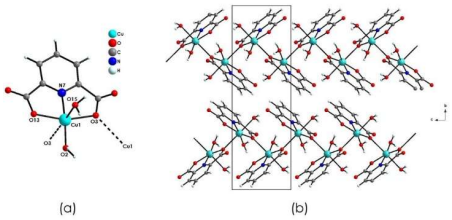

Figure 7. (a) molecular unit of **3** with important labels; (b) projection along the a-axis of the unit-cell of $\{Cu(DPA)(H_2O)_2\}_n$ chains running along the c-axis of the unit-cell.

The behavior of the Tb-Xo4 complex is completely different. The automated crystallization experiments revealed that all drops remained perfectly homogeneous, without any sign of precipitation at 10 mM concentration. At 100 mM, only 3 conditions over 576 led to the formation of micro-crystalline precipitate (Figures S1-3). These conditions contain among other ammonium fluoride, calcium acetate or ammonium sulfate in the presence of polyethylene glycol. The obtained microcrystals did not present optimal quality for X-ray diffraction and we have been unable to reproduce them in larger batch for the preparation of well diffracting crystals. After several crystallization attempts, we hardly get TbXo4 crystals of global formula $[Tb_4L_4(H_2O)_4]Cl_4 \bullet 15H_2O$ (**4**) from slow evaporation of a water/acetonitrile mixture (Tables S3, S9 and S10). These crystals are luminescent in the green upon UV irradiation (Figure 8). In the structure, one Tb(III) atom is coordinated in a {N5O4} environment. The deprotonated ligand L is coordinated by two oxygen atoms from the carboxylate moieties and five nitrogen ones from the pyridine and the triazacyclononane macrocycle. The Tb-O bond lengths (2.403 Å) are shorter than Tb-N ones (2.566 Å) and are in good agreement with those previously reported in the literature for identical complexes.[41] The coordination sphere is completed by the two oxygen atoms from one water molecule with Tb-O bond length (2.449 Å) comparable to other Tb-O(L) ones and one oxygen atom from the carbonyl fragment belonging to the ligand of a neighboring complex with a short Tb-O bond (2.265 Å). Thus, four complexes assemble in a remarkable tetrameric supramolecular architecture (Figure 8). The charge balance is assumed by the presence of four Cl^- anions within the unit-cell. Fifteen non-coordinated water molecules also co-crystallize within the unit-cell. Both of these non-coordinated molecules or anions are located in canals running along the c-axis of the unit-cell and generated by the global complexes packing.

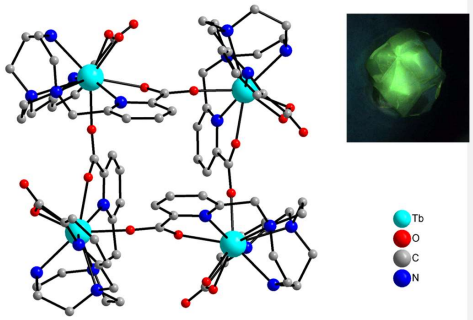

Figure 8. Structure of complex **4**. For clarity, hydrogen atoms and non-coordinated chloride and water molecules have been removed. In inset is reported the picture of one crystal of complex **4** under UV irradiation (λ_{ex} = 254 nm).

In addition, the stability experiments in solution have been performed with Tb-Xo4, in the same conditions than those with $[Na]_3[Eu(DPA)_3]$. Firstly, addition of 1 eq. of MCl_2 to a Tb-Xo4 solution led to a much slower decrease of the green luminescence observed over several days (Figure S5) compared to the almost instantaneous luminescence decrease observed $[Na]_3[Eu(DPA)_3]$ (Figure S4). Secondly, in the presence of alkaline-earth salts ($MgCl_2$, $CaCl_2$, $BaAc_2$ 1-10 eq), no variation of the luminescence intensity of Tb-Xo4 was observed for days (Figure S6). All results indicated that a trans-metalation reaction occurs between the two lanthanide complexes and transition metal cations but with a very different kinetic underlining a higher stability for the macrocyclic Tb-Xo4 complex. In addition, in the presence of alkaline-earth salts, Tb-Xo4 is highly stable whereas $[Eu(DPA)_3]^{3-}$ precipitates and/or self-crystallizes.

Conclusion.

In conclusion, in this article we started undertaking the systematic analysis of the influence of the commercial crystallization kit composition on the efficiency of two lanthanide based additives: $[Na]_3[Eu(DPA)_3]$ and Tb-Xo4. This study reveals that the tris-dipicolinate complex presents a lower chemical stability and a strong tendency to self-crystallization detrimental for its use in high-throughput robotized crystallization platform. On the other hand, the Tb-Xo4 is perfectly soluble in the crystallization media, stable in the presence of alkaline-earth dications and slowly decomposed (within days) by trans-metalation with transition metals. This article also revealed the potential positive of interactions between the crystallization mixture component and Tb-Xo4 leading to the formation of more complex adducts like {AdkA/Tb-Xo4/Mg^{2+}/GOL} or {FprA/Tb-Xo4/Ca^{2+}/GOL} in the protein binding sites. The observation of such multi-components adducts illustrated the complexity and versatility of the supramolecular chemistry occurring at the surface of proteins. The role of such adducts during the crystallization process is currently under investigation.

Acknowledgements.

Authors acknowledge the Fondation Maison de la Chimie, Agence Nationale de la Recherche (ANR Ln23 -13-BS07-0007-01) and SATT Pulsalys for grants to AR, SE and SDP and Region AuRA for financial support (program Xo4-2.0). Authors also thank the Polyvalan Company for its help and the pôle de compétitivité Lyon-Biopôle.

Keywords. Protein crystallography • lanthanide complexes • triazacyclononane • picolinate

References.

1. Terwilliger, T. C.; Stuart, D.; Yokoyama, S., Lessons from Structural Genomics. *Annual Rev. Biophys.* **2009,** *38* (1), 371-383.
2. Khurshid, S.; Saridakis, E.; Govada, L.; Chayen, N. E., Porous nucleating agents for protein crystallization. *Nat. Protoc.* **2014,** *9* (7), 1621-1633.
3. Khurshid, S.; Saridakis, E.; Govada, L.; Chayen, N. E., Porous nucleating agents for protein crystallization. *Nat Protoc* **2014,** *9* (7), 1621-33.
4. Santarsiero, B. D.; Yegian, D. T.; Lee, C. C.; Spraggon, G.; Gu, J.; Scheibe, D.; Uber, D. C.; Cornell, E. W.; Nordmeyer, R. A.; Kolbe, W. F.; Jin, J.; Jones, A. L.; Jaklevic, J. M.; Schultz, P. G.; Stevens, R. C., An approach to rapid protein crystallization using nanodroplets. *J. Appl. Crystallogr.* **2002,** *35*, 278-281.
5. Brown, J.; Walter, T. S.; Carter, L.; Abrescia, N. G. A.; Aricescu, A. R.; Batuwangala, T. D.; Bird, L. E.; Brown, N.; Chamberlain, P. P.; Davis, S. J.; Dubinina, E.; Endicott, J.; Fennelly, J. A.; Gilbert, R. J. C.; Harkiolaki, M.; Hon, W. C.; Kimberley, F.; Love, C. A.; Mancini, E. J.; Manso-Sancho, R.; Nichols, C. E.; Robinson, R. A.; Sutton, G. C.; Schueller, N.; Sleeman, M. C.; Stewart-Jones, G. B.; Vuong, M.; Welburn, J.; Zhang, Z.; Stammers, D. K.; Owens, R. J.; Jones, E. Y.; Harlos, K.; Stuart, D. I., A procedure for setting up high-throughput nanolitre crystallization experiments. II. Crystallization results. *J. Appl. Crystallogr.* **2003,** *36*, 315-318.
6. Hendrickson, W. A., Anomalous diffraction in crystallographic phase evaluation. *Quarterly Reviews of Biophysics* **2014,** *47* (1), 49-93.
7. Doublié, S., [29] Preparation of selenomethionyl proteins for phase determination. In *Methods Enzymol.*, Academic Press: 1997; Vol. 276, pp 523-530.
8. D'Arcy, A.; Mac Sweeney, A.; Haber, A., Using natural seeding material to generate nucleation in protein crystallization experiments. *Acta Crystallogr. Section D-Biol. Crystallogr.* **2003,** *59*, 1343-1346.
9. Georgieva, D. G.; Kuil, M. E.; Oosterkamp, T. H.; Zandbergen, H. W.; Abrahams, J. P., Heterogeneous nucleation of three-dimensional protein nanocrystals. *Acta Crystallogr. Section D-Biol.Crystallogr.* **2007,** *63*, 564-570.
10. Saridakis, E.; Khurshid, S.; Govada, L.; Phan, Q.; Hawkins, D.; Crichlow, G. V.; Lolis, E.; Reddy, S. M.; Chayen, N. E., Protein crystallization facilitated by molecularly imprinted polymers. *Proc. Nat. Ac. Sci.* **2011,** *108* (27), 11081.
11. Khurshid, S.; Govada, L.; El-Sharif, H. F.; Reddy, S. M.; Chayen, N. E., Automating the application of smart materials for protein crystallization. *Acta Crystallogr. Section D-Struct.Biol.***2015,** *71*, 534-540.
12. Bijelic, A.; Rompel, A., The use of polyoxometalates in protein crystallography - An attempt to widen a well-known bottleneck. *Coord. Chem. Rev.* **2015,** *299*, 22-38.
13. Breibeck, J.; Bijelic, A.; Rompel, A., Transition metal-substituted Keggin polyoxotungstates enabling covalent attachment to proteinase K upon co-crystallization. *Chem Commun* **2019,** *55* (77), 11519-11522.
14. Mac Sweeney, A.; Chambovey, A.; Wicki, M.; Muller, M.; Artico, N.; Lange, R.; Bijelic, A.; Breibeck, J.; Rompel, A., The crystallization additive hexatungstotellurate promotes the crystallization of the HSP70 nucleotide binding domain into two different crystal forms. *PLoS One* **2018,** *13* (6), e0199639.
15. Bijelic, A.; Rompel, A., Polyoxometalates: more than a phasing tool in protein crystallography. *ChemTexts* **2018,** *4* (3), 10.
16. McGovern, R. E.; Fernandes, H.; Khan, A. R.; Power, N. P.; Crowley, P. B., Protein camouflage in cytochrome c-calixarene complexes. *Nat Chem* **2012,** *4* (7), 527-33.
17. McGovern, R. E.; Feifel, S. C.; Lisdat, F.; Crowley, P. B., Microscale Crystals of Cytochrome c and Calixarene on Electrodes: Interprotein Electron Transfer between Defined Sites. *Angew. Chem. Int. Ed.* **2015,** *54* (21), 6356-9.
18. Guagnini, F.; Antonik, P. M.; Rennie, M. L.; O'Byrne, P.; Khan, A. R.; Pinalli, R.; Dalcanale, E.; Crowley, P. B., Cucurbit[7]uril-Dimethyllysine Recognition in a Model Protein. *Angew. Chem., Int. Ed.* **2018,** *57* (24), 7126-7130.
19. Engilberge, S.; Rennie, M. L.; Dumont, E.; Crowley, P. B., Tuning Protein Frameworks via Auxiliary Supramolecular Interactions. *ACS Nano* **2019,** *13* (9), 10343-10350.
20. Pompidor, G.; D'Aleo, A.; Vicat, J.; Toupet, L.; Giraud, N.; Kahn, R.; Maury, O., Protein crystallography through supramolecular

interactions between a lanthanide complex and arginine. *Angew. Chem. Int. Ed.* **2008,** *47* (18), 3388-91.
21. Talon, R.; Kahn, R.; Dura, M. A.; Maury, O.; Vellieux, F. M.; Franzetti, B.; Girard, E., Using lanthanoid complexes to phase large macromolecular assemblies. *J Synchrotron Radiat* **2011,** *18* (1), 74-8.
22. Engilberge, S.; Riobe, F.; Di Pietro, S.; Lassalle, L.; Coquelle, N.; Arnaud, C. A.; Pitrat, D.; Mulatier, J. C.; Madern, D.; Breyton, C.; Maury, O.; Girard, E., Crystallophore: a versatile lanthanide complex for protein crystallography combining nucleating effects, phasing properties, and luminescence. *Chem Sci* **2017,** *8* (9), 5909-5917.
23. Engilberge, S.; Wagner, T.; Santoni, G.; Breyton, C.; Shima, S.; Franzetti, B.; Riobe, F.; Maury, O.; Girard, E., Protein crystal structure determination with the crystallophore, a nucleating and phasing agent. *J. Appl. Crystallogr.* **2019,** *52* (Pt 4), 722-731.
24. de Wijn, R.; Hennig, O.; Roche, J.; Engilberge, S.; Rollet, K.; Fernandez-Millan, P.; Brillet, K.; Betat, H.; Morl, M.; Roussel, A.; Girard, E.; Mueller-Dieckmann, C.; Fox, G. C.; Olieric, V.; Gavira, J. A.; Lorber, B.; Sauter, C., A simple and versatile microfluidic device for efficient biomacromolecule crystallization and structural analysis by serial crystallography. *IUCrJ* **2019,** *6* (Pt 3), 454-464.
25. Rempel, S.; Colucci, E.; de Gier, J. W.; Guskov, A.; Slotboom, D. J., Cysteine-mediated decyanation of vitamin B12 by the predicted membrane transporter BtuM. *Nat. Comm.* **2018,** *9* (1), 3038.
26. Hajj Chehade, M.; Pelosi, L.; Fyfe, C. D.; Loiseau, L.; Rascalou, B.; Brugière, S.; Kazemzadeh, K.; Vo, C.-D.-T.; Ciccone, L.; Aussel, L.; Couté, Y.; Fontecave, M.; Barras, F.; Lombard, M.; Pierrel, F., A Soluble Metabolon Synthesizes the Isoprenoid Lipid Ubiquinone. *Cell Chem. Biol.* **2019,** *26* (4), 482-492.e7.
27. Roche, J.; Girard, E.; Mas, C.; Madern, D., The archaeal LDH-like malate dehydrogenase from Ignicoccus islandicus displays dual substrate recognition, hidden allostery and a non-canonical tetrameric oligomeric organization. *J. Struct. Biol.* **2019,** *208* (1), 7-17.
28. Schada von Borzyskowski, L.; Severi, F.; Krüger, K.; Hermann, L.; Gilardet, A.; Sippel, F.; Pommerenke, B.; Claus, P.; Cortina, N. S.; Glatter, T.; Zauner, S.; Zarzycki, J.; Fuchs, B. M.; Bremer, E.; Maier, U. G.; Amann, R. I.; Erb, T. J., Marine Proteobacteria metabolize glycolate via the β-hydroxyaspartate cycle. *Nature* **2019,** *575* (7783), 500-504.
29. Belot, L.; Ouldali, M.; Roche, S.; Legrand, P.; Gaudin, Y.; Albertini, A. A., Crystal structure of Mokola virus glycoprotein in its post-fusion conformation. *PLOS Pathogens* **2020,** *16* (3), e1008383.
30. Bernhardsgrütter, I.; Vögeli, B.; Wagner, T.; Peter, D. M.; Cortina, N. S.; Kahnt, J.; Bange, G.; Engilberge, S.; Girard, E.; Riobé, F.; Maury, O.; Shima, S.; Zarzycki, J.; Erb, T. J., The multicatalytic compartment of propionyl-CoA synthase sequesters a toxic metabolite. *Nat. Chem. Biol.***2018,** *14* (12), 1127-1132.
31. Vogeli, B.; Engilberge, S.; Girard, E.; Riobe, F.; Maury, O.; Erb, T. J.; Shima, S.; Wagner, T., Archaeal acetoacetyl-CoA thiolase/HMG-CoA synthase complex channels the intermediate via a fused CoA-binding site. *Proc Natl Acad Sci* **2018,** *115* (13), 3380-3385.
32. Engilberge, S.; Riobe, F.; Wagner, T.; Di Pietro, S.; Breyton, C.; Franzetti, B.; Shima, S.; Girard, E.; Dumont, E.; Maury, O., Unveiling the Binding Modes of the Crystallophore, a Terbium-based Nucleating and Phasing Molecular Agent for Protein Crystallography. *Chem. Eur; J.* **2018,** *24* (39), 9739-9746.
33. Zhao, X.-Q.; Zuo, Y.; Gao, D.-L.; Zhao, B.; Shi, W.; Cheng, P., Syntheses, Structures, and Luminescence Properties of a Series of LnIII−BaIIHeterometal-Organic Frameworks. *Cryst. Growth & Des.* **2009,** *9* (9), 3948-3957.
34. Chen, Y.; Li, L.; Zhang, Q.; Liu, S.; Tian, Z.; Ju, Z., Effects of calcium ions on crystal structure and luminescence properties of six rare earth metal complexes. *J. Solid State Chem.* **2020,** *281*, 121053.
35. Chen, Y.; Zhao, X.; Gao, R.; Ruan, Z.; Lin, J.; Liu, S.; Tian, Z.; Chen, X., Temperature-induced solvent assisted single-crystal-to-single-crystal transformation of Mg(II)-Ln(III) heterometallic coordination polymers. *J. Solid State Chem.* **2020,** *292*, 121674.
36. Tancrez, N.; Feuvrie, C.; Ledoux, I.; Zyss, J.; Toupet, L.; Le Bozec, H.; Maury, O., Lanthanide Complexes for Second Order Nonlinear Optics: Evidence for the Direct Contribution of f Electrons to the Quadratic Hyperpolarizability. *J. Am. Chem. Soc.* **2005,** *127* (39), 13474-13475.
37. D'Aleo, A.; Pompidor, G.; Elena, B.; Vicat, J.; Baldeck, P. L.; Toupet, L.; Kahn, R.; Andraud, C.; Maury, O., Two-photon microscopy and spectroscopy of lanthanide bioprobes. *Chemphyschem* **2007,** *8* (14), 2125-32.
38. D'Aléo, A.; Toupet, L.; Rigaut, S.; Andraud, C.; Maury, O., Guanidinium as powerful cation for the design of lanthanate tris-dipicolinate crystalline materials: Synthesis, structure and photophysical properties. *Opt. Mater.* **2008,** *30* (11), 1682-1688.
39. Mooibroek, T. J.; Gamez, P.; Pevec, A.; Kasunic, M.; Kozlevcar, B.; Fu, W. T.; Reedijk, J., Efficient, stable, tunable, and easy to synthesize, handle and recycle luminescent materials: [H2NMe2]3[Ln(III)(2,6-dipicolinolate)3] (Ln = Eu, Tb, or its solid solutions). *Dalton Trans* **2010,** *39* (28), 6483-7.
40. Sileo, E. E.; Rigotti, G.; Rivero, B. E.; Blesa, M. A., Kinetic study of the thermal dehydration of copper(II) dipicolinates: Crystal and molecular structure of Cu(II) (Pyridine 2,6-Dicarboxylato) DI- and Trihydrated. *J. Phys. Chem. Solids* **1997,** *58* (7), 1127-1135.
41. Nocton, G.; Nonat, A.; Gateau, C.; Mazzanti, M., Water Stability and Luminescence of Lanthanide Complexes of Tripodal Ligands Derived from 1,4,7-Triazacyclononane: Pyridinecarboxamide versus Pyridinecarboxylate Donors. *Helv. Chim. Acta* **2009,** *92* (11), 2257-2273.